

SNGR based fast analysis of slat track noise sources

Wenhu Wang^{1,2}, Qinchao Wang¹, Cyrille Breard¹, Yifeng Sun¹

¹ Shanghai Aircraft Design and Research Institute

² Key Laboratory of Aerodynamic Noise Control

Abstract

SNGR based fast analysis are conducted to evaluate the broadband noise sources of slat, track and cavity. The strongest noise source of the slat locates at the impingement point of the vortical shear flow on the downstream cove surface. The track brings new strong noise source above the track root and the leading edge of the main wing. The cavity further introduces large scale strong noise source in the separation zone above the cavity. Compared with transient noise source results, SNGR method successfully captures the main features of all three configurations.

Keywords: SNGR, slat track, track cavity, noise source

1. Introduction

Three major noise sources of civil airliners are engines, landing gears and high-lift devices. For single-aisle airliners, high-lift device noise prevails over landing gear noise, while slat noise and slat track noise are the first and second biggest components of high-lift device noise[1]. The slat track and the accompanying cavity do not only redistribute the vortex strength in the slat cove, but also change the path of the near field acoustic propagation, resulting in a significant high frequency noise increment[2].

The hybrid numerical method is the state of art of aero-acoustic simulations, which treats the physics of aerodynamic noise as two separate processes[3]: 1) noise source generation, usually solved by DES-based transient simulation in order to capture the near field turbulent details; 2) far field noise propagation, usually solved by FW-H acoustic analogy in order to model the acoustic radiation. For a single high-lift simulation case, the DES/FW-H hybrid method demands dozens of million mesh cells, along with several weeks for a converged result, which may struggle to follow the fast paces of industrial design cycles. SNGR (Stochastic Noise Generation and Radiation) is a fast analysis method of broadband noise sources[4], which creates the stochastic fluctuations of noise source items, by utilizing the averaged turbulent information from RANS-based simulation. SNGR does not apply to all kinds of tone noise[1], which appear in aero-acoustic wind tunnel tests, including the high frequency tone due to slat trailing edge vortex shedding, the high frequency tone due to T-S instability on slat suction side, as well as the low frequency tone due to laminar flow separation at slat cusp. However, as a Reynolds number effect, all the tones above do not exist in the flight tests of real aircrafts. Both slat noise and slat track noise of a full size airliner are broadband noise, which can be analyzed by SNGR method.

By using the commercial code ANSYS FLUENT, this paper compares the noise sources results of steady and transient simulations, in order to investigate if SNGR can provide a good enough prediction.

2. Model and Mesh

An unswept three-element high-lift wing is chosen for analysis, with a stowed chord of 3m, a span of 0.8m, a Mach number of 0.2, as well as an angle of attack of 6 degrees. As shown in Figure 1, near field noise sources are compared for three configurations with different leading edge: 1) slat; 2) slat and track; 3) slat, track and cavity.

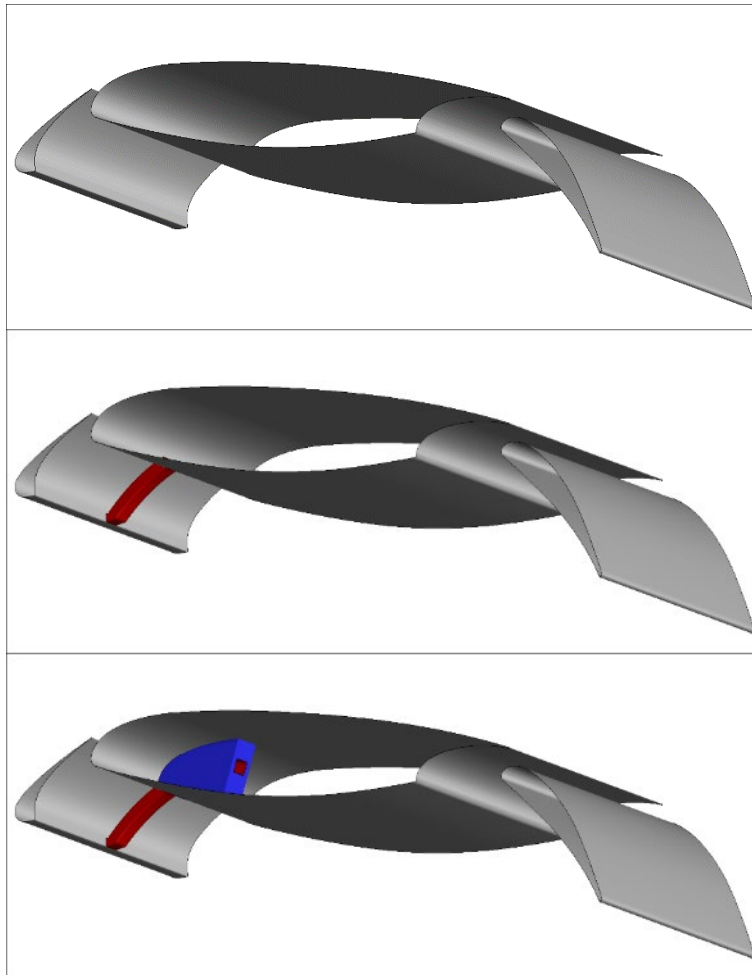
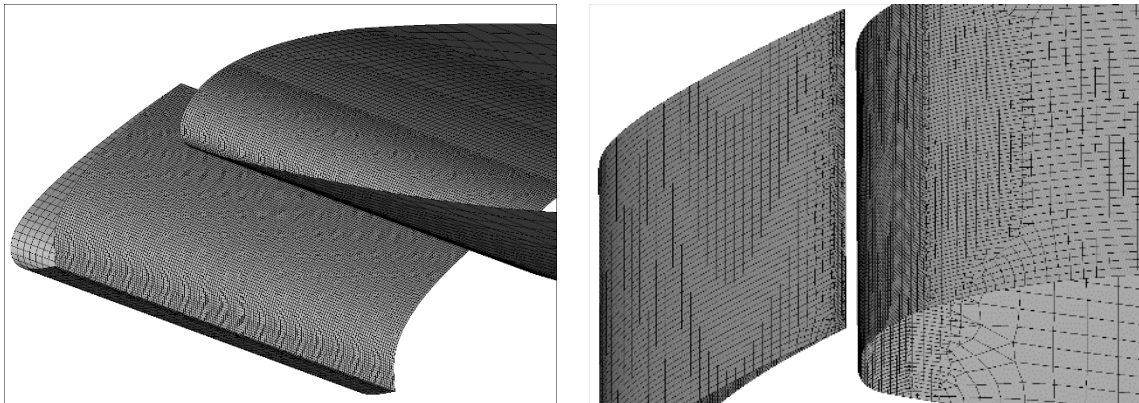


Figure 1 – three configurations (track in red, cavity in blue).

By using the commercial software Pointwise, quad-dominant unstructured surface mesh is paved, while hexahedral-dominant boundary layer mesh is extruded by T-Rex function. As shown by Figure 2, the finest surface mesh are allocated in the slat gap area, including slat cove surface, slat track surface, cavity surface, as well as the leading edge surface of main wing, in order to resolve the main surface noise sources.



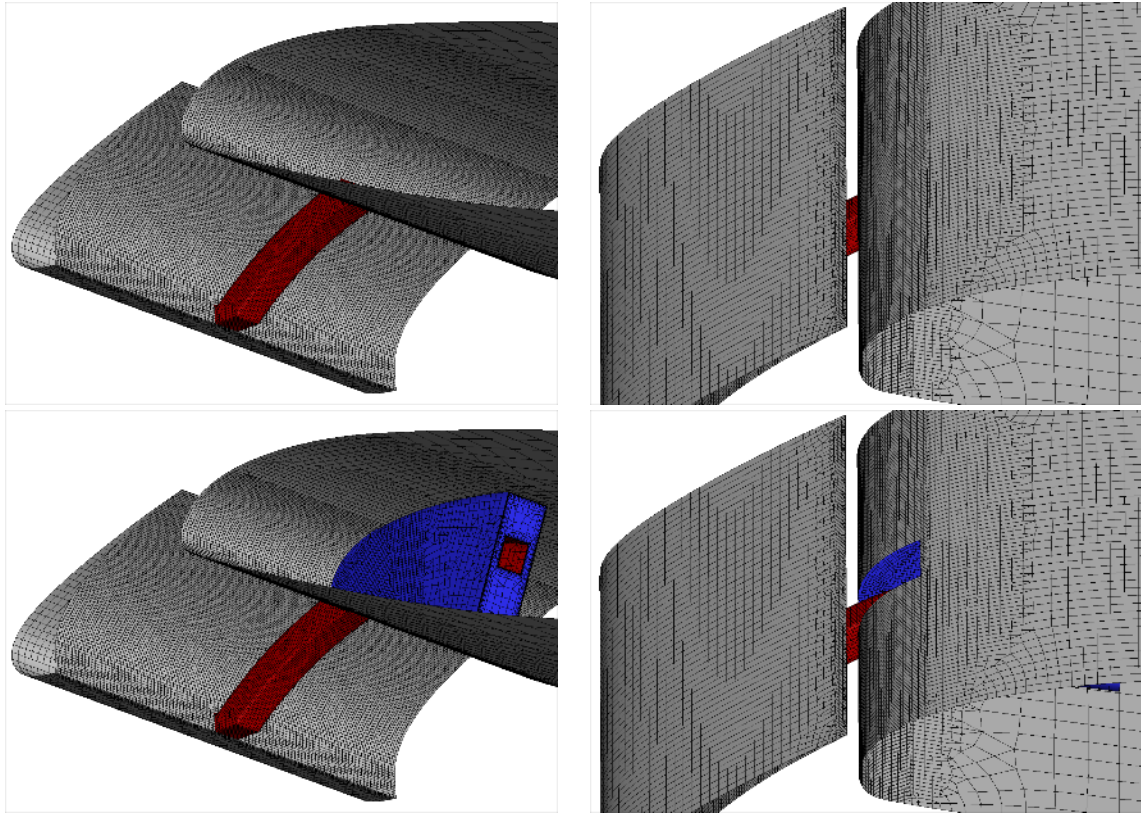


Figure 2 – surface mesh of three configurations.

As shown by Figure 3, the space source function is used to refine the volume mesh of slat cove area, slat gap area and cavity area, in order to resolve the main volume noise sources.

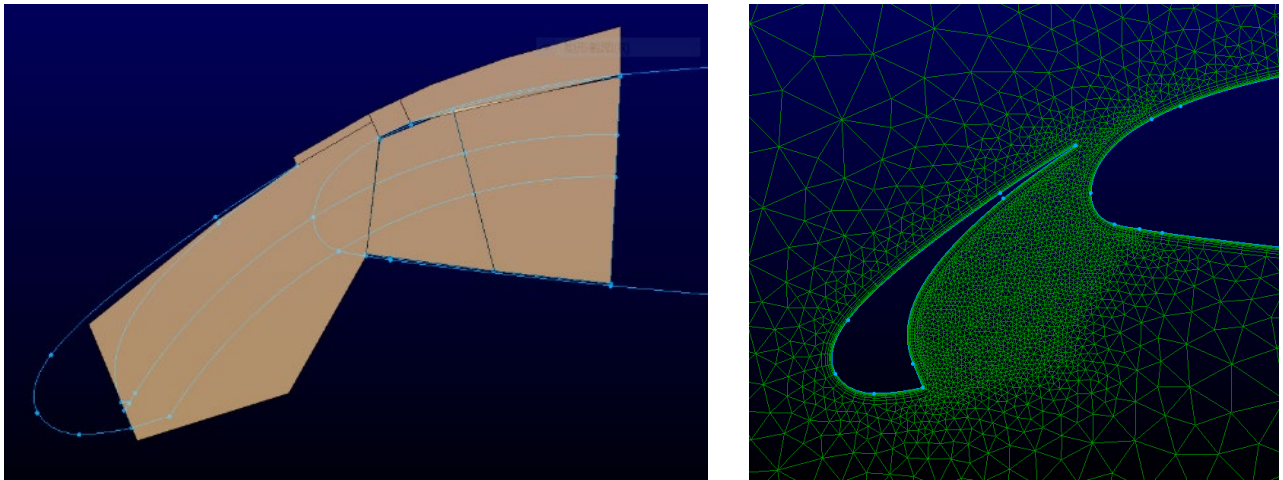


Figure 3 – volume mesh refinement.

3. Flow Field of Steady Simulation

Steady simulations are conducted by using RANS solver of ANSYS FLUNET. The solver formulation is density-based implicit. The flux type is Roe-FDS. The spatial discretization scheme is third-order MUSCL. Turbulent model is SST $k-\omega$ model. The CASM technique is used to accelerate the convergence rate of the high aspect ratio boundary layer mesh, while FMG initialization technique is used to prevent unexpected divergence accompanied with CASM.

Figure 4 compares the steady C_p and streamlines of three configurations in the spanwise plane $z=0$ (symmetry plane). Compared with the baseline configuration, slat track splits the flow structure of the slat cove recirculation area into two parts, while track cavity induces three big vortices structures.

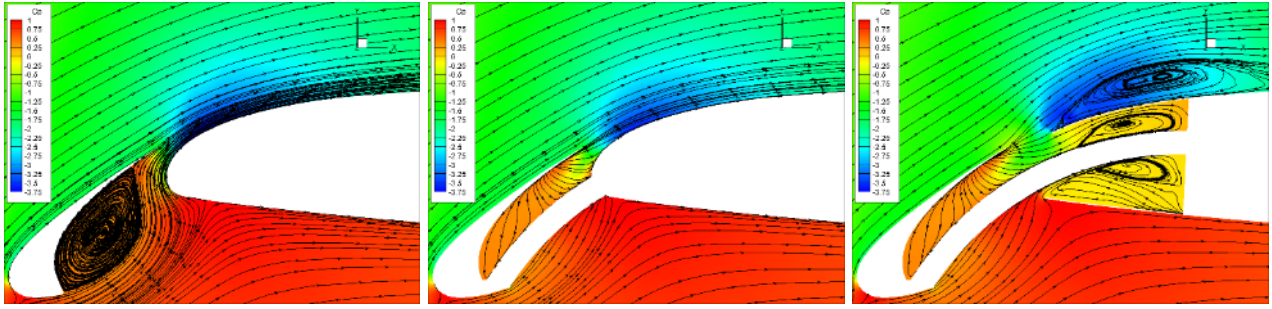


Figure 4 – steady flow field of three configurations in plane $z=0$.

Figure 5 compares the steady C_p and streamlines of three configurations in the spanwise plane $z=0.036\text{m}$. Compared with the baseline configuration, slat track compresses the flow structure of the slat cove recirculation area, while the two vortices inside track cavity merge into one bigger vortex.

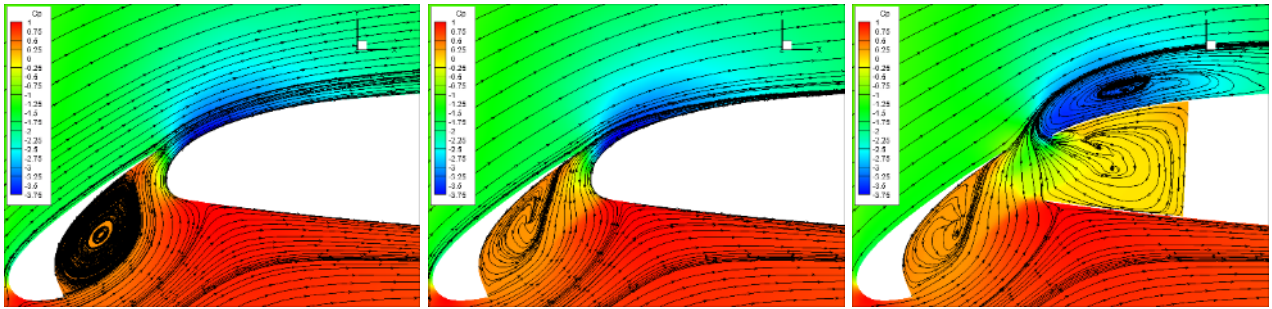


Figure 5 – steady flow field of three configurations in plane $z=0.036\text{m}$.

Figure 6 compares the steady C_p and streamlines of three configurations in the spanwise plane $z=0.1\text{m}$. Slat track's influence on the slat cove recirculation area has been very limited, while track cavity still creates extra separation area on the upper surface of main wing.

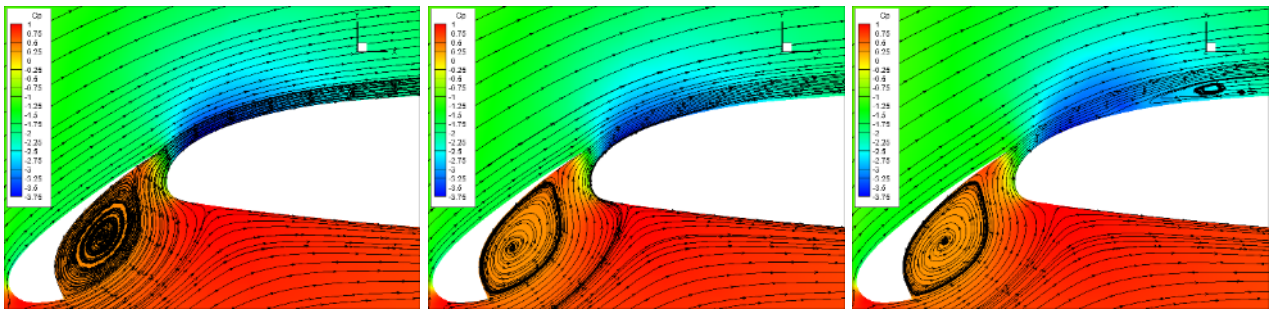


Figure 6 – steady flow field of three configurations in plane $z=0.1\text{m}$.

Figure 7 compares the steady C_p and streamlines of three configurations in the spanwise plane $z=0.2\text{m}$. Neither slat track nor track cavity can reshape the typical slat flow structure, so that all three configurations perform similar.

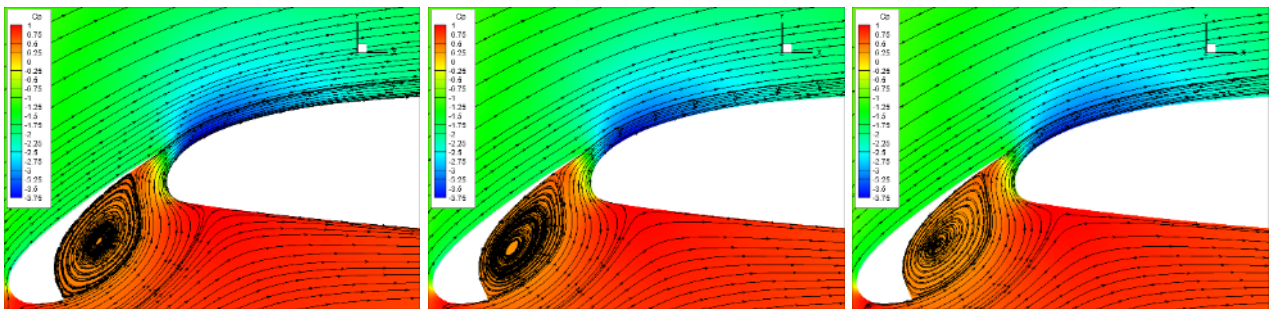


Figure 7 – steady flow field of three configurations in plane $z=0.2\text{m}$.

4. Flow Field of Transient Simulation

Transient simulations are conducted by using DDES solver of ANSYS FLUNET. The temporal discretization scheme is second-order implicit. Turbulent model is SST-based DDES model. The time step size is 10^{-5}s . The steady RANS results are used as the initial value of transient simulations.

Figure 8 compares the transient z-vorticity of three configurations in the spanwise plane $z=0$ (symmetry plane). Compared with the baseline configuration, slat track breaks the main slat cove recirculation structure into many small vortices, while track cavity induces big vortices structures internally and on the upper surface of main wing.

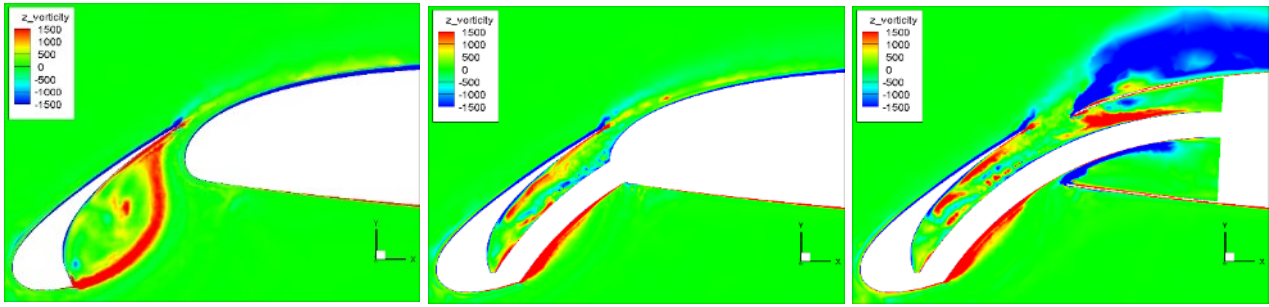


Figure 8 – transient flow field of three configurations in plane $z=0$.

Figure 9 compares the transient z-vorticity of three configurations in the spanwise plane $z=0.036\text{m}$. Compared with the baseline configuration, slat track induces extra vortex structure on the leading edge of main wing, while track cavity brings strong vortices mixing effect internally.

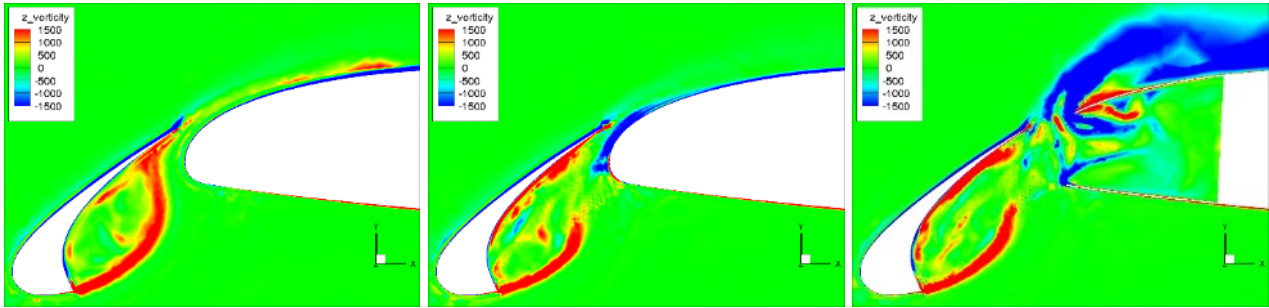


Figure 9 – transient flow field of three configurations in plane $z=0.036\text{m}$.

Figure 10 compares the transient z-vorticity of three configurations in the spanwise plane $z=0.1\text{m}$. Compared with the baseline configuration, slat track only has minor influence on the upper surface of main wing, while track cavity still makes a difference.

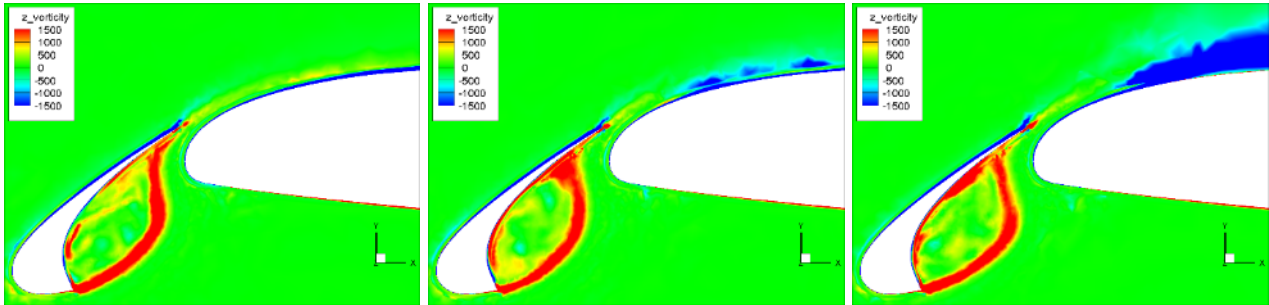


Figure 10 – transient flow field of three configurations in plane $z=0.1\text{m}$.

Figure 11 compares the transient z-vorticity of three configurations in the spanwise plane $z=0.2\text{m}$. Neither slat track nor track cavity can reshape the typical slat flow structure, so that all three configurations perform similar.

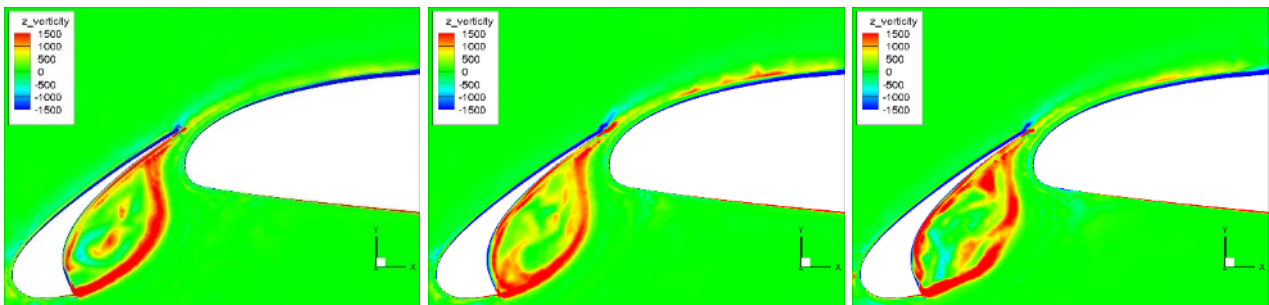


Figure 11 – transient flow field of three configurations in plane $z=0.2\text{m}$.

5. Comparison of Steady and Transient Noise Sources

Based on the flow field results above, steady and transient noise sources are compared. Steady noise sources are evaluated by SNGR method, which creates the stochastic fluctuations of noise source items, by utilizing the averaged turbulent information from RANS-based simulation. On the other hand, transient noise sources are evaluated as the divergence of Lamb vector, which is the cross product of transient vorticity vector and transient velocity vector.

Figure 12 compares the steady and transient noise sources of three configurations in the spanwise plane $z=0$ (symmetry plane). According to the transient results, the strongest noise source of baseline locates at the impingement point of the vortical shear flow on the downstream cove surface, which follows the current consensus. Slat track brings new strong noise source above the track root and the leading edge of the main wing, while track cavity further introduces large scale strong noise source in the separation zone above the cavity. All the main features above are successfully captured by SNGR method.

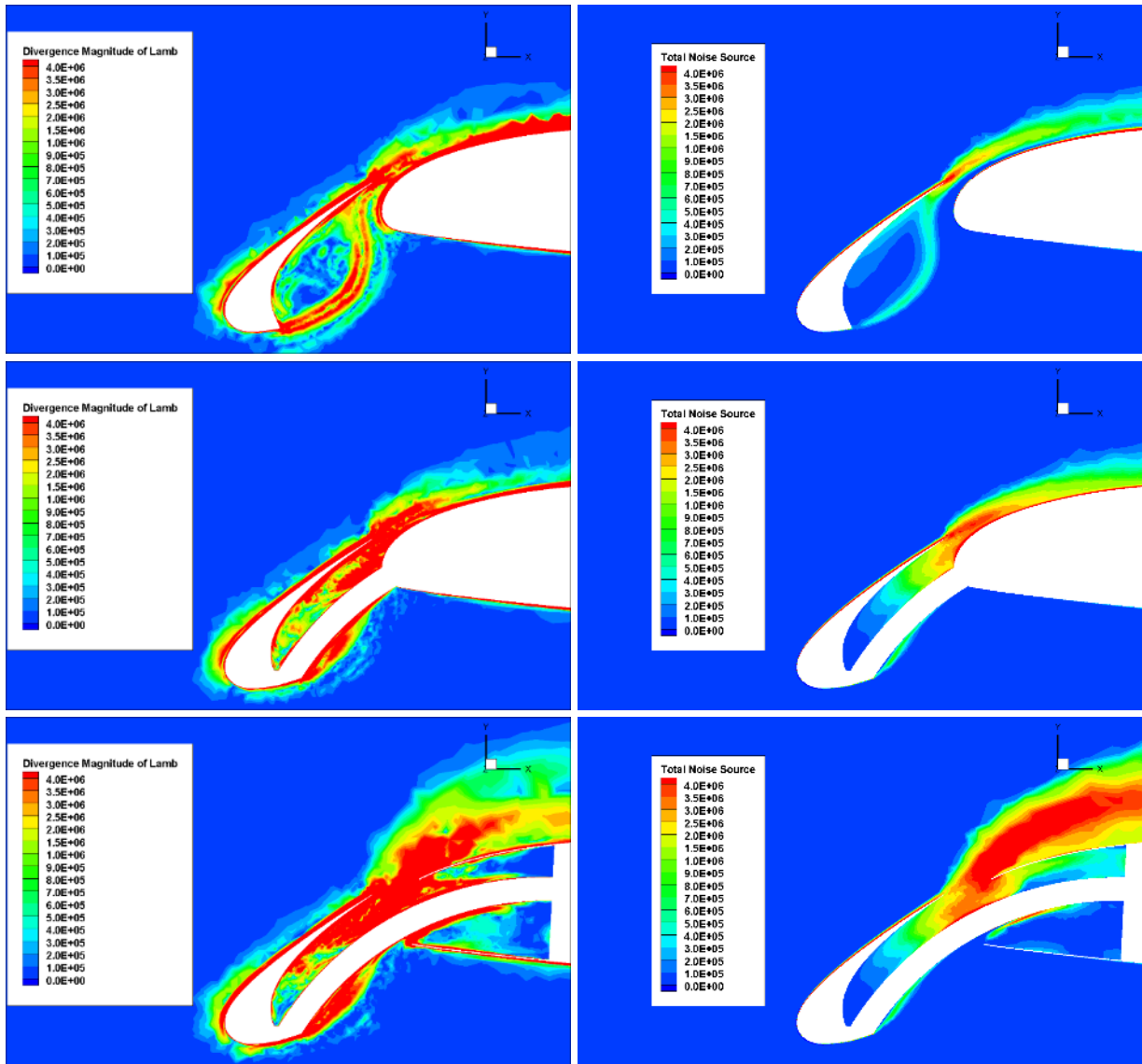


Figure 12 – transient (left) and steady (right) noise sources comparison in plane $z=0$.

Figure 13 compares the steady and transient noise sources of three configurations in the spanwise plane $z=0.036m$. Due to the closeness to the symmetry plane, the transient noise sources of all three configurations distribute similar as in the symmetry plane. Moreover, the vacant spaces of slat track are also filled by strong noise sources. SNGR method also performs well.

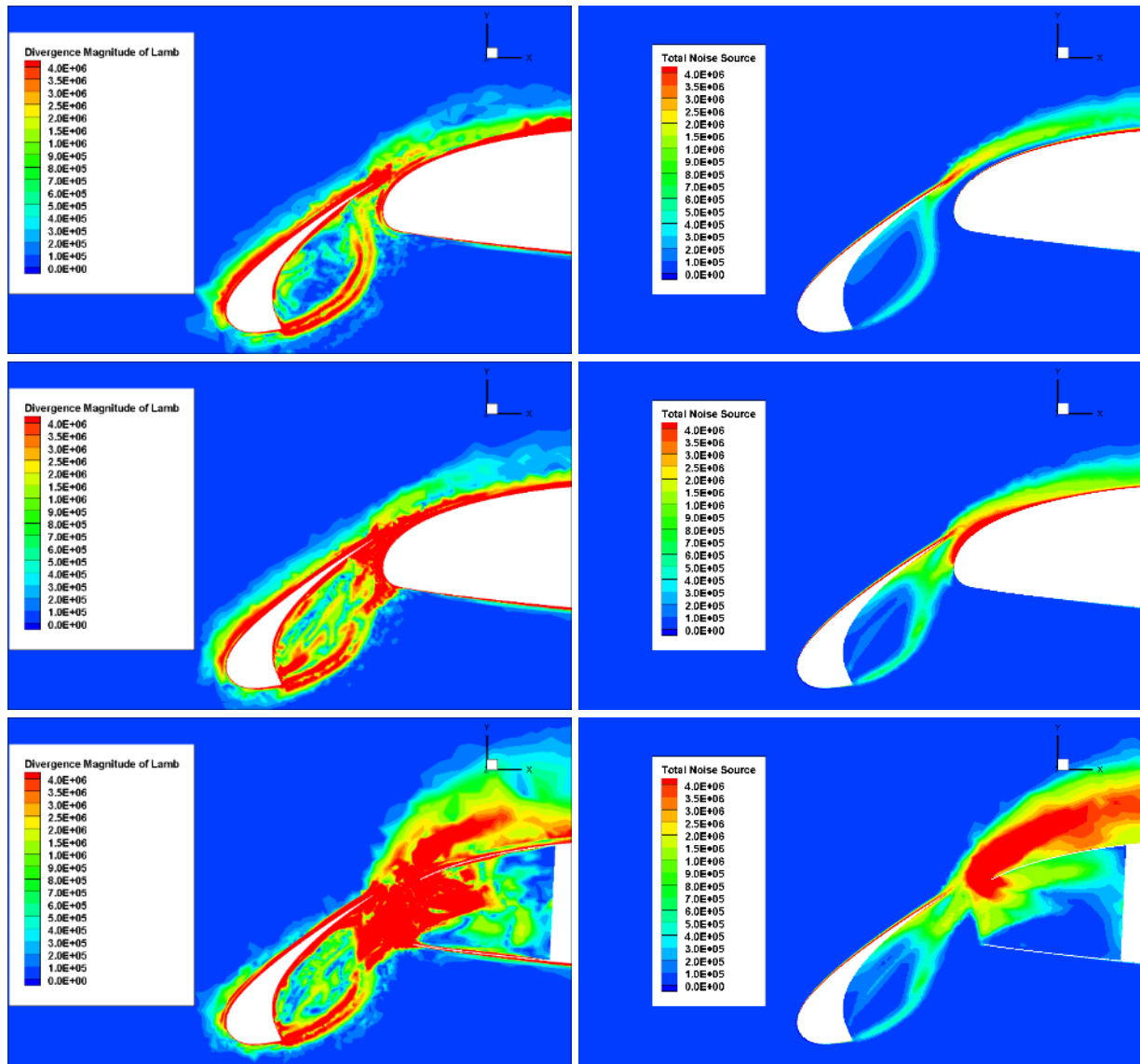
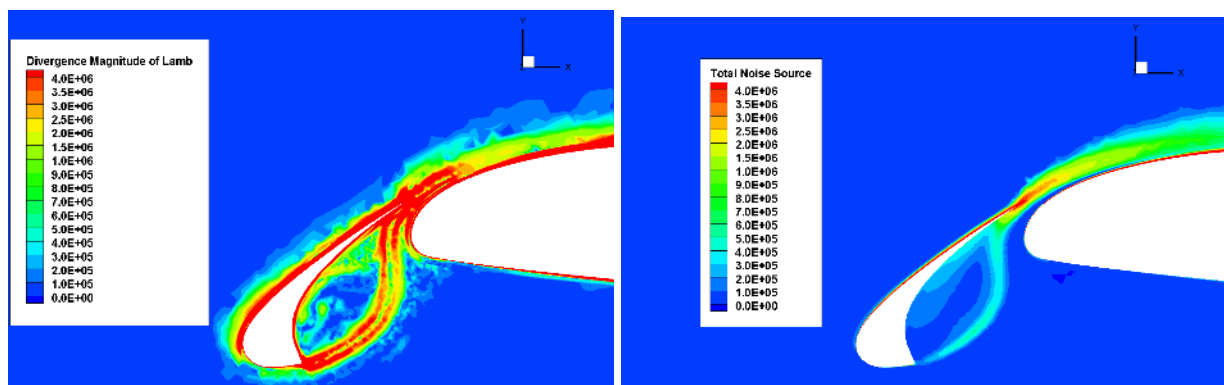


Figure 13 – transient (left) and steady (right) noise sources comparison in plane $z=0.036m$.

Figure 14 compares the steady and transient noise sources of three configurations in the spanwise plane $z=0.1m$. Both slat track and track cavity create extra noise sources on the upper surface of main wing, so that the summation effect is stronger than slat track only. SNGR method reflects the summation effect well.



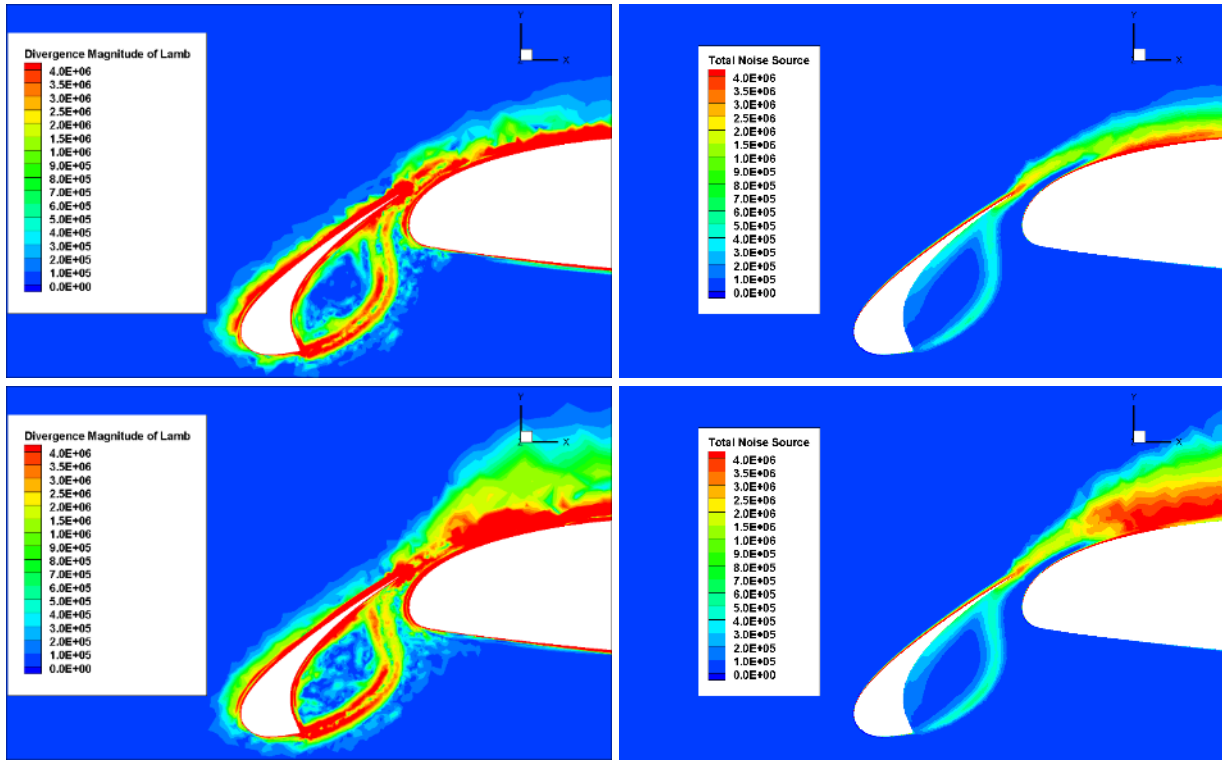
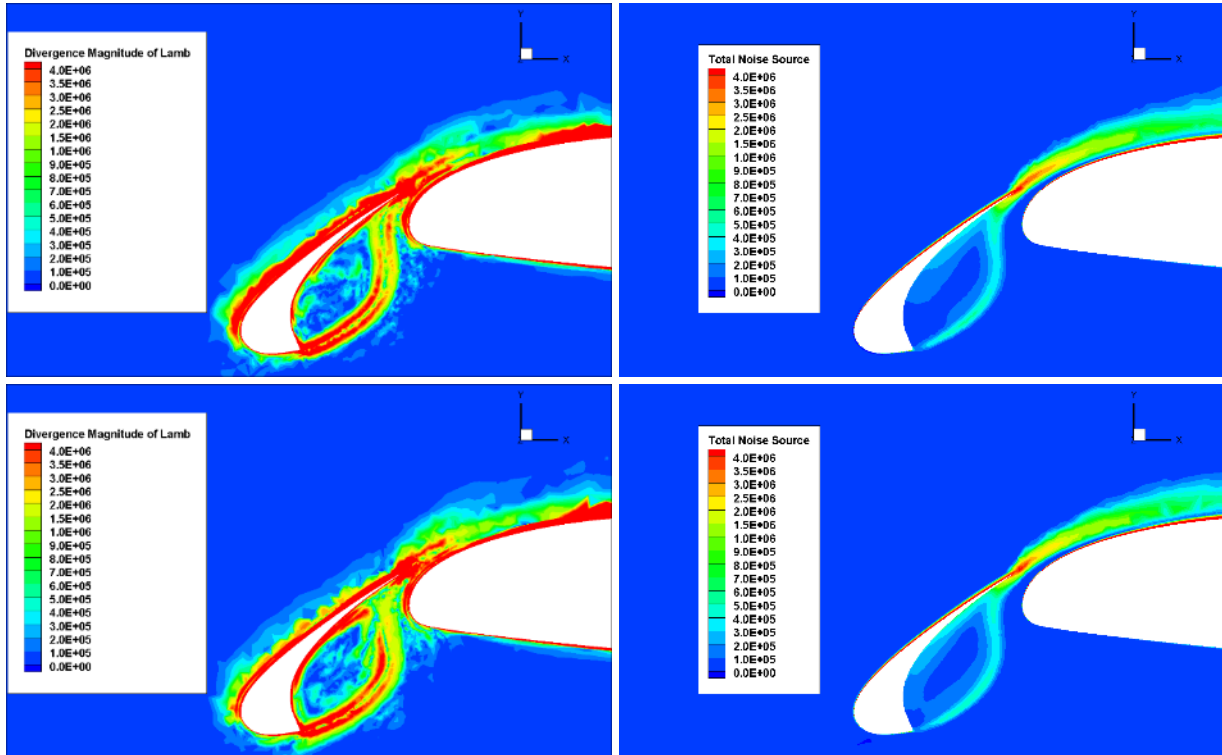


Figure 14 – transient (left) and steady (right) noise sources comparison in plane $z=0.1\text{m}$.

Figure 15 compares the steady and transient noise sources of three configurations in the spanwise plane $z=0.2\text{m}$. Both steady and transient results of all three configurations show similar distributions, since this plane is far enough from the track and the cavity.



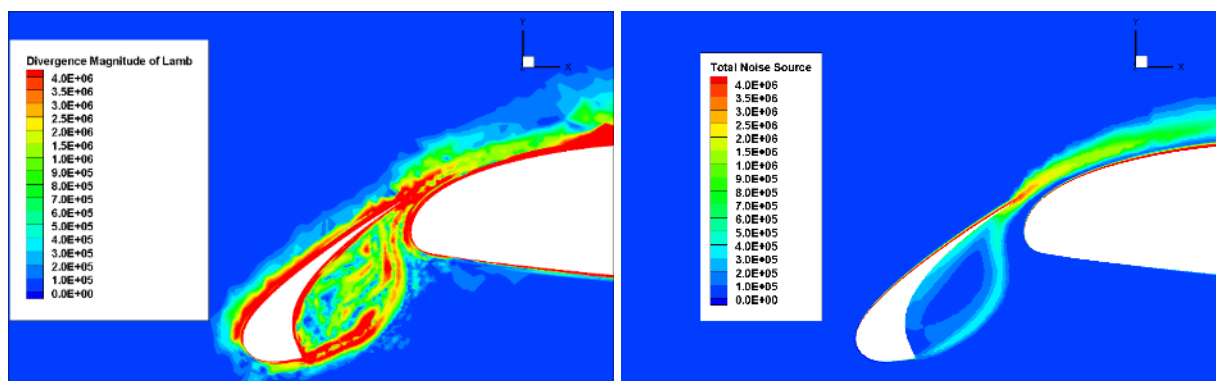


Figure 15 – transient (left) and steady (right) noise sources comparison in plane $z=0.2\text{m}$.

6. Conclusion

SNGR based fast analysis are conducted to evaluate the broadband noise sources of slat, track and cavity. The strongest noise source of the slat locates at the impingement point of the vortical shear flow on the downstream cove surface. The track brings new strong noise source above the track root and the leading edge of the main wing. The cavity further introduces large scale strong noise source in the separation zone above the cavity. Compared with transient noise source results, SNGR method successfully captures the main features of all three configurations.

7. Acknowledgements

This work is sponsored by Shanghai Sailing Program (18YF1429600) and Key Laboratory of Aerodynamic Noise Control Program (ANCL20190111).

8. Contact Author Email Address

wangwenhu1@comac.cc

9. Copyright Statement

The authors confirm that they, and/or their company or organization, hold copyright on all of the original material included in this paper. The authors also confirm that they have obtained permission, from the copyright holder of any third party material included in this paper, to publish it as part of their paper. The authors confirm that they give permission, or have obtained permission from the copyright holder of this paper, for the publication and distribution of this paper as part of the ICAS proceedings or as individual off-prints from the proceedings.

References

- [1] Dobrzynski W. Almost 40 years of airframe noise research: what did we achieve?. *Journal of Aircraft*, Vol. 47, No. 2, pp 353-367, 2010.
- [2] Wang X. *Computational aeroacoustic study of aircraft slat tracks and cut-outs*. PhD thesis, University of Southampton, 2013.
- [3] Redonnet S. Aircraft noise prediction via aeroacoustic hybrid methods development and application of ONERA tools over the last decade: some examples. *ONERA Aerospace Lab Journal*, Vol. 7, No. 7, pp 1-16, 2014.
- [4] Ewert R and Emunds R. CAA slat noise studies applying stochastic sound sources based on solenoidal digital filters. *11th AIAA/CEAS Aeroacoustics Conference*, Monterey, CA, USA, Vol. 1, AIAA 2005-2862, pp 1-23, 2005.